2011

Fabrication and Preliminary Characterization of Hydrophobic Silica Aerogel Films for Oil Remediation Studies

Ellen Yang
Pomona College

POMONA COLLEGE

Fabrication and Preliminary Characterization of Hydrophobic Silica Aerogel Films for Oil Remediation Studies

Ellen Yang

In partial fulfillment of a Bachelor of Arts Degree in Environmental Analysis
Pomona College, Claremont, California
Academic Year: 2010 – 2011
Advisor: Malkiat S. Johal

Table of Contents

Abstract

Due to the potential of oil sorbents for oil spill clean-up, hydrophobic silica-based aerogel thin films have been synthesized and characterized by various methods. Aerogels were prepared using a two-step acid/base sol-gel process and functionalized with trimethylchlorosilane in hexane, followed by drying in ambient conditions. After film deposition by spin-coating, samples were characterized by scanning electron microscopy, nitrogen adsorption analysis (BET surface area = 377.66 m^2/g), and variable-angle spectroscopic ellipsometry (thickness of 287.00 ± 0.85 nm, refractive index of 1.08, porosity of 80.9%). Unlike previous studies with aerogel films, quartz crystal microbalance with dissipation monitoring (QCM-D) was applied to preliminarily measure the oil absorbing capacity of the fabricated aerogels. Upon exposure to hexadecane, aerogel films retained the model oil with an estimated Sauerbrey mass of ~970.6 ng/cm^2. These initial investigations suggest that oil adsorption-desorption studies with hydrophobic aerogel thin films can be further explored with QCM-D.

List of Figures

1. Introduction

After an estimated 172 million gallons of oil gushed into the Gulf of Mexico, the BP oil spill of 2010 has replaced the Exxon Valdez oil spill of 1989 (10.8 million gallons) as the largest accidental oil spill in the history of the petroleum industry.[1] Oil spills pose an environmental threat to various ecosystems. Moreover, the long-term effects of environmental pollution have demonstrated the need to advance efforts to protect coastline and marine environments.[2] In the attempt to salvage marine and wildlife habitats, a wide range of materials have been utilized, though not always successfully, for oil spill clean-up and recovery.[2] Future response strategies should therefore apply oil recovery methods that aim to eliminate or reduce the short- and long-term consequences of oil pollution. This begins by improving oil treatment processes that aim to contain and clean up oil-impacted areas.

Common materials used during oil recovery include booms, skimmers, absorbents, dispersants, and solidifiers.[2] Booms are floating barriers that physically confine the oil to a specific area for recovery or prevent it from entering a given area.[2] Once the booms corral a specific site, skimmers attempt to mechanically extract the oil layer from the water surface for disposal or reuse. This method does not completely separate oil from water. Absorbents, however, collect and separate oil from water by absorption. Rather than separating oil from water, dispersants accelerate the dispersal of floating oil into the water column by forming water-soluble micelles.[2] With sufficient wave action, smaller oil droplets may form and scatter over a larger volume of water, where biodegradation may be enhanced.[2] Solidifiers can also be used to transform the oil into a solid. These dry, granular hydrophobic polymers react with the oil to form a tight, cohesive mass that stays afloat and can be easily removed.[3]

A disadvantage of solidifiers is their tendency to non-selectively cross-link with other hydrocarbons in the vicinity, including weeds and other organic matters.[3]

Compared to other materials, absorbents are advantageous for oil remediation because of their potential to collect and completely extract oil from the spill site.[2] Aside from being recyclable and biodegradable, the ideal adsorbent would exhibit hydrophobicity and oleophilicity, maximize uptake capacity and rate of uptake, increase retention over time, and recover oil.[2] The various types of oil-sorbents can be classified into three categories: inorganic mineral products, synthetic organic products, and organic vegetable products.[2] Inorganic materials encompass zeolites, graphite, silica, and sorbent clay.[2] Synthetic organic products include polypropylene and polyurethane foams, both of which are the most widely used commercial oil-sorbents.[2] A downside to these hydrophobic and oleophilic polymeric materials is that they degrade more slowly in comparison to mineral or vegetable products.[2] Additionally, these materials are not as sustainable in nature or as naturally occurring as inorganic mineral products. Vegetable products, which include natural fiber, straw, and peat moss, have demonstrated poor buoyancy, low oil uptake capacity, and low hydrophobicity.[4] When we consider the overall impact of clean-up methods, inorganic mineral products seem to possess the greatest potential as effective oil-sorbents for ecological recovery.

Silica exhibits several properties associated with the ideal oil-sorbent material. When turned into hydrophobic silica aerogels, these inert, non-toxic, and sustainable products have potential commercial applications in oil spill clean-up operations'[5,6] The purpose of this study is to synthesize and monitor hydrophobic aerogels as possible absorbent materials for oil removal from contaminated water systems.

1.1. Silica Aerogels

Discovered by Kistler[7] in 1931, silica aerogels are low-density (3 kg/m^3), highly porous (~99%) solid networks of a gel that are typically derived from sol-gel chemistry.[8] These mesoporous (2-50 nm pores) foams filled with air have unique properties, including low refractive indices (<1.1), low dielectric constants (<1.7), low thermal conductivity (0.01-0.015 W/m·K), and low sound velocities (<100 m/s). As a result, aerogels have been used in a wide range of industrial applications, including heat-storage, thermal insulation, acoustics, and catalysis.[9,10,11]

1.2. Mechanism of Sol-Gel Reaction

Silica gels are produced using the sol-gel method through three reactions: hydrolysis, water condensation, and alcohol condensation (Figure 1). During hydrolysis, a silicon alkoxide reacts with water to form silicic acid, $Si(OH)_4$ in the presence of a mutual solvent:

$$Si(OR)_4 + 4H_2O \leftrightarrow Si(OH)_4 + 4ROH \quad [1]$$

R denotes an alkyl, vinyl, or aryl group.[2,7] An alcohol (ROH) is often the preferred solvent for circumventing transesterification reactions. A mineral acid (e.g. HCl) or base (e.g. NH_4OH) is generally used as a catalyst to enhance the extremely slow rate of reaction from 4×10^{-6} L mol^{-1} s^{-1} at neutral pH to 6×10^{-3} L mol^{-1} s^{-1}at pH 1.2.[12] The reactive silanol groups will form a siloxane bridge (Si-O-Si) either with each other or an alkoxide (Si-OR) group by releasing water or alcohol:

$$2Si(OR)_4 \leftrightarrow (OR)_3Si - O - Si(OR)_3 + H_2O \quad [2]$$

$$(OR)_3Si - OR + HO - Si(OR)_3 \leftrightarrow (OR)_3Si - O - Si(OR)_3 + ROH \quad [3]$$

Since the tetravalent silicon atom can form up to four siloxane bridges, further polycondensation will occur. As shown in Figure 1, a network of silica nanoparticles (SiO_4-tetrahedra) will eventually form throughout the sol.[2] Silicon atoms with a terminal hydroxyl group or alkoxide group will cover the surface of the network. When enough nanoparticles span the liquid medium, a porous gel forms and viscosity increases considerably.[13]

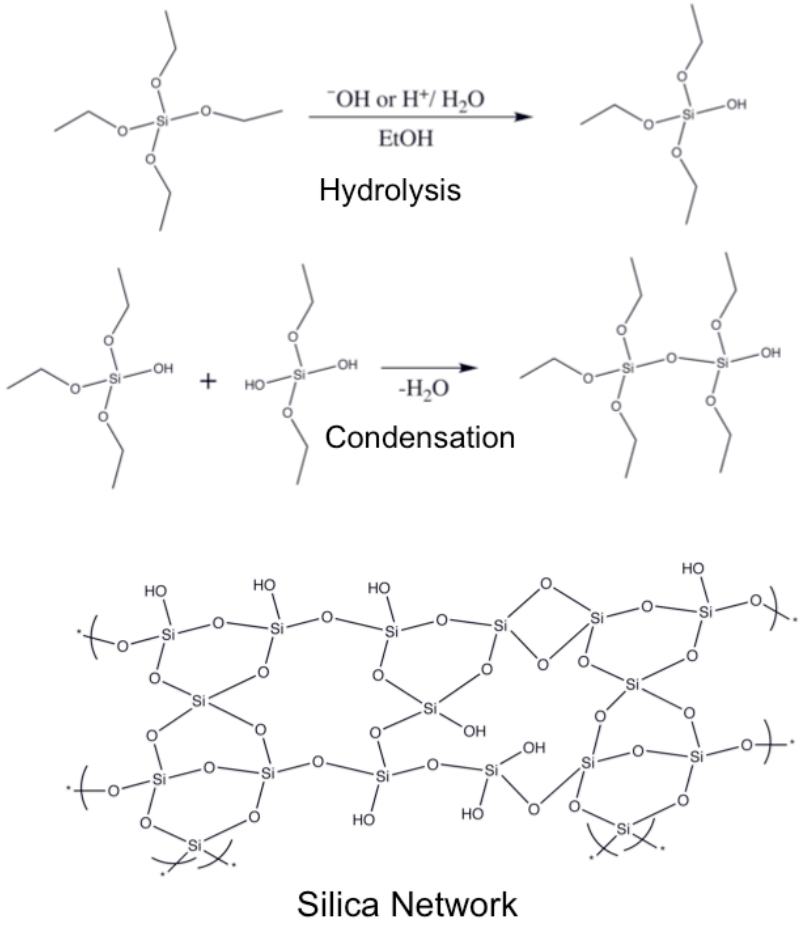

Figure 1. Sol-gel reactions during silica network formation: hydrolysis, condensation, and polymerization.

Sol-gels are synthesized according to the type of properties desired. The porosity and density of the synthesized aerogel depends on various parameters, including temperature, pH, and catalysts.[2] Sol-gels can be produced by a single-step ("one-pot") or a two-step method.

The final form of silica gels is largely influenced by the pH of the solution.[5] In the first method, either an acid or a base catalyst is incorporated into the silica precursor-alcohol-water mixture. At low pH (highly acidic), silica particles tend to undergo hydrolysis by forming straight chains with low cross-link density.[5] An acid catalyst will therefore produce a soft gel that is easy to re-solubilize. At high pH (highly basic), polymerization increases and the number of cross-links between polymers increases as well.[5] A basic catalyst would promote polymerization and expand the silica network. Compared to the one-step process, the two-step method increases the rate of condensation and reduces gelation time. During the two-step acid-base catalyzed sol-gel process,[14] a pre-polymerized silica alkoxide (e.g. tetraethoxysilane, TEOS) is prepared under acidic conditions and re-dissolved under basic conditions.

Single-step and two-step aerogels possess slightly different properties. Although single-step aerogels are mechanically stronger, two-step aerogels are optically clearer due to their narrower pore size and pore distribution.[15] Once a gel develops, pore impurities (i.e. catalyst, solvent, water) can be extracted through multiple washings in pure solvent. In most cases, the solvent is an alcohol. During the purification process, the alcogel may undergo further chemical reactions. This process of aging stiffens and strengthens the silica skeleton.[16]

1.3. Surface Functionalization of Silica Aerogels

To complete the aerogel process, liquid must be removed from the pores without collapsing the silica skeleton. After gelation, the alcogels contain a number of unreacted silanol groups on their surface. When liquid molecules contained within the pores volatilize, liquid volume decreases, increasing surface tension at the solid-liquid interface. Large

capillary forces induce gel shrinkage and gel cracking.[17] Since surface tension will pull against any structures adhering to the liquid, we must eliminate these compressive forces. The liquid enclosed within the pores can be extracted through two methods: 1) supercritical drying, and 2) solvent evaporation.[2]

1.3.1. Supercritical Drying Method

The process of supercritical drying is a common method used to remove the liquid trapped in a gel's pores without inducing gel shrinkage.[2] During this process, the alcogel is subcritically dried in an autoclave.[6] Kistler created the first aerogels by initially raising the pressure and then the temperature above the liquid's critical point.[7] Beyond this point, the liquid behaves more like a fluid, and the liquid-vapor interface ceases to exist.[18] Capillary forces are eliminated.[2] As the system cools, the fluid is expelled from the aerogel and replaced by a low density gas such as carbon dioxide. Although supercritical drying is effective against capillary stress, the extreme conditions are not suitable for thin film deposition.[19]

1.3.2. Solvent Evaporation Method

In comparison, solvent evaporation is a cost-effective, safe, and continuous method of drying.[2,17] Brinker developed an ambient pressure drying method that reduces surface tension through the chemical modification of the hydrophilic gel surface.[20] These wet aerogels can be functionalized with non-polar groups to inhibit further reactions with water vapor in the air. Hydrophobic reagents, including β-diketonates, alcohol amines and carboxylic acids, will replace the H from a surface silanol (Si-OH) group with a non-polar alkyl or aryl group (Figure 2).[19] When using solvent extraction, the functionalized gel can be dried without significant shrinkage because the interior surface of the pores will no longer be predisposed

to condensation reactions. Any drying-related shrinkage during the final stage of aerogel synthesis is essentially reversible in the absence of capillary stress, allowing the porosity of the film to expand, or spring-back, to its wet size.[21]

a)

b)

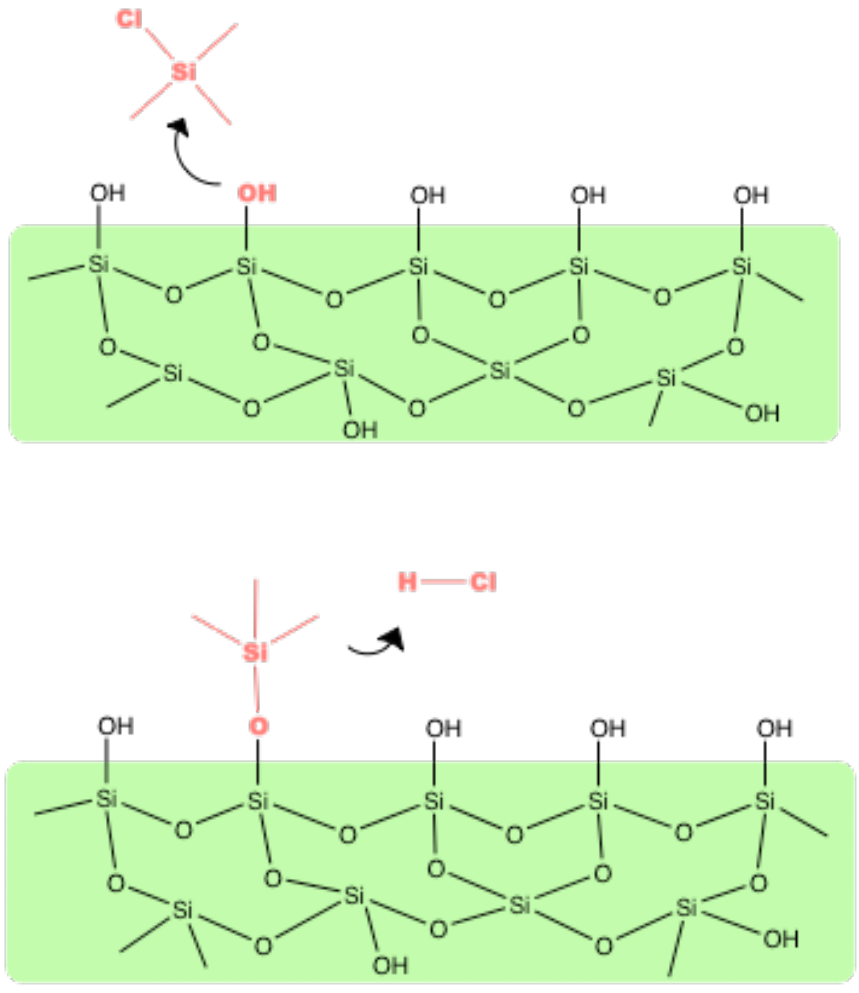

Figure 2. Mechanism for surface silylation with trimethylchlorosilane (TMCS):
a) nucleophilic oxygen in alcohol group attacks the silicon atom in TMCS, b) silanol group is functionalized and hydrochloric acid is the leaving group.

1.4. Methods of Characterization

The physical properties of the aerogel can be characterized with the use of various analytical techniques.[22]

1.4.1. Scanning Electron Microscopy (SEM)

Scanning electron microscopy (SEM) can be used to study the microstructure of aerogels. The SEM emits a high-energy beam of electrons that interacts with atoms on or near the surface of the sample. The various signals produced can provide quantitative information about an aerogel's topography, including its cracking behavior, relative thickness and pore size distribution.[2]

1.4.2. Ellipsometry

Variable-angle spectroscopic ellipsometry (VASE) is another technique often used to determine film thickness. The ellipsometer measures the change in polarization after a polarized laser beam strikes the sample surface. Due to the weak mechanical strength and light scattering of aerogels, SEM is often the preferred method of characterization.[23] Ellipsometry can also be employed to measure the refractive index of the films.[24] Based on the relationship between porosity (π) and index of refraction (n),[21] the porosity of the silica aerogel films can be calculated as follows:

$$\pi = \left[\frac{1.455 - n_D}{1.455 - n_A}\right] \qquad [4]$$

where 1.455 is the theoretical index of refraction for SiO_2, n_D is the measured refractive index of the porous film, and n_A is the refractive index of air (n_A = 1.000).

1.4.3. Gas-Phase Adsorption

The specific surface area of the aerogel can be determined by gas-phase adsorption.[25] During this process, an inert gas, such as nitrogen gas, is adsorbed onto the surface of a solid material. For porous aerogels, the adsorbate will cover the surface of the pores as well. Various models have been proposed to account for this phenomenon. Langmuir first developed a simple, yet effective model in 1916. The Langmuir adsorption isotherm expresses the relationship between the pressure of the gas and the moles of gas adsorbed onto a solid surface.[26] The model assumes that the gas molecules form a monolayer on the adsorbent at saturation and that a strong interaction exists between the molecules and the adsorbent. Based on the Langmuir relation, the surface area of the aerogel can be determined.

The Langmuir model for monolayer coverage is invalid at high gas pressures (i.e. at high surface coverage).[27] Under these conditions, the initial adsorbate layer can act as the new substrate surface, allowing additional adsorption to occur beyond saturation. A more advanced model must therefore be applied to factor in multi-layer adsorption.

Developed by Brunauer, Emmett, and Teller (BET) in 1938, the BET theory takes into account multi-layer gas adsorption and the interaction between binding sites.[27] It is an extension of the Langmuir theory.

$$\Theta = \frac{n}{n_{mon}} = \frac{cz}{\{(1-z)[1-(1-c)z]\}} \qquad [5]$$

Θ = fraction of total coverage, n = number of moles of adsorbed gas, n_{mon}= number of moles of gas required to form a monolayer, c = constant, p^* = vapor pressure of the gas, $z = p/p^*$ and p = partial pressure of the gas.

In the limit of low pressure (p = 1), the BET isotherm simplifies to the Langmuir isotherm if we equate constant c to equilibrium constant K multiplied by p*. A linear form of the BET equation can be obtained and tested by the method of least squares:

$$\frac{z}{(1-z)n} = \frac{1}{cn_{mon}} + \left(\frac{c-1}{cn_{mon}}\right)z \qquad [6]$$

By determining n_{mon} from the linearized BET isotherm plot, the specific surface area (S) of the aerogel can be calculated from the following relation:

$$S = n_{mon}\sigma N_A \qquad [7]$$

where σ = molecular cross-section for the gas and N_A = Avogadro's number. The pore size distribution in the aerogel can also be determined from the BET isotherm.[20] It is important to note that BET theory does not provide an accurate reflection of the true surface area. However, it is easy to use and widely accepted.

1.4.4. Quartz Crystal Microbalance with Dissipation (QCM-D)

Quartz crystal microbalance with dissipation monitoring (QCM-D) could prove useful for the characterization of aerogel films. Sauerbrey's work in 1959 first recognized the possibility of using quartz crystal microbalance (QCM) technology to monitor mass uptake in vacuum.[28] The acoustic sensing technique can detect very small changes in the amount of material that is either adsorbed or desorbed from a surface.

QCM consists of a piezoelectric quartz crystal sandwiched between a pair of electrodes. Upon the sensor's connection to an oscillator and AC voltage, the quartz crystal will oscillate at its resonance frequency (f). The frequency of the oscillating crystal decreases with adsorption of material. Based on the linear relationship between a decrease in frequency

(Δf) and mass adsorbed (Δm), the Sauerbrey relation can be used to determine the adsorbed mass of thin and rigid films.[28]

$$\Delta m = -\frac{C \cdot \Delta f}{n} \qquad [8]$$

C = 17.7 ng Hz^{-1} cm^{-2} is the sensitivity factor for a 5 MHz quartz crystal and n = 1,3,5,… is the overtone number.

The Sauerbrey relation becomes invalid when the film is not rigid. In such cases, the Sauerbrey relation would underestimate the mass of the adsorbing film. We would need to apply a viscoelastic model to determine the structural properties of the soft film. Unlike conventional QCMs, QCM-Ds are capable of fully characterizing floppy, non-rigid films. They are not restricted to the gas phase but can be applied to liquid mediums. Aside from measuring changes in frequency, QCM-Ds account for the energy loss of the oscillator, or dissipation (D). Changes in the dissipation parameter (ΔD) provide viscoelastic information about the adsorbed films.[29]

As a powerful tool for studying nanoscale interactions on different surfaces, QCM-D is potentially useful for characterizing aerogel thin films. At present, however, the investigation of aerogel thin films using QCM-D has not been exploited. QCM-D work in this field has been limited to monitoring the adsorption and evolution of vesicles on xerogel thin films.[30]

1.5. Oil Absorption Studies

Previous studies have done extensive work on the oil absorption properties of silica aerogels in bulk. Reynolds and co-workers determined that a supercritically dried CF_3-aerogel absorbed 40 to 140 times more oil than a non-functionalized silica aerogel in

simulated oil-spill clean up conditions.[31] When an oil to aerogel ratio of 3.5 was maintained in an oil and salt-water mixture, the CF_3-aerogel separated the oil from the water. Additional oil absorption and desorption studies with superhydrophobic aerogels demonstrated that these materials had a very high uptake capacity, were removable from the contaminated system, and reusable without inducing structural changes.[32] Rao *et al* determined that the rate of absorption was a function of the density and the surface tension of the organic liquid, whereas the rate of desorption relied upon the vapor pressure and the surface tension of the respective liquid. His team used transmission electron microscopy to image microstructural changes in the aerogel sample before and after absorption of organic liquids.

A less studied phenomenon is the absorption and desorption of oils in hydrophobic aerogel thin films. Coronado *et al* has demonstrated the selective absorbance of oil from water by solid support materials, such as fiberglass, alumina, and cotton wool, when coated with CF_3-modified aerogel films.[33] Silylation can also occur with trimethylchlorosilane (TMCS). Lee and his team developed an ambient drying process that utilizes a solvent exchange/modification agent consisting of isopropyl alcohol (IPA), TMCS and *n*-Hexane to produce superhydrophobic aerogels.[34] Prakash has also derivatized silica films in TMCS and hexane.[19] Maximum film porosity was optimized in hydrophobic silica films that were prepared at ambient pressure and heated to 450°C to yield refractive indices between 1.006-1.036 (equivalent porosity 98.5%-91%) with thicknesses varying from 0.1 to 3.5 μm, depending on the concentration of the sol and dip-coating rate.[19] Other studies have also applied pyrolysis at 450°C to enhance porosity of silica-based aerogel thin films from 60% to more than 90%.[20] These films were deposited onto silicon wafers by dip-coating and spin-coating processes.

1.6. Purpose

The aim of this study is to extend previous work on the preparation of silica-based aerogel thin films and develop a model system for investigating the oil absorbing capabilities of synthesized silica thin films using QCM-D. This model system will utilize oil-water emulsions and pure oil to simulate basic conditions during oil spills.

Emulsions often contain an emulsifier that stabilizes the interface between oil and water droplets. Surface-active agents (surfactants), which constitute one class of emulsifiers, can be used to increase the kinetic stability of the oil-water droplets over time by incorporating hydrophobic molecules into surfactant micelles.[35] Poly(oxyethylene)sorbitan monolaurate (Tween 20), a nonionic surfactant, has been used to lower the interfacial tension between hexadecane and water.[35]

The QCM-D can monitor the interaction between the aerogels and the emulsions. Unlike other analytical tools, QCM-D can provide time-resolved mass changes in the film. These systems, however, traditionally rely on AT-cut quartz crystal sensors that limit thin-film monitoring to below approximately 300ºC.[36] Since the piezoelectric constant of quartz drops sharply above this temperature, the synthesized films cannot undergo supercritical extraction or pyrolysis. It is therefore necessary to fabricate a hydrophobic silica aerogel film that not only fits the criteria for QCM analysis but also proves effective in oil-contaminated water.

2. Experimental

Over the course of this study, a series of aerogels were synthesized both indirectly and directly (Figure 3). Each batch of aerogels will be referred to by "generation." Aerogels were initially prepared indirectly, or prior to thin film deposition. The experimental protocol was slightly modified to accommodate the direct synthesis of a thin film aerogel.

All silicate sols were derived using a two-step acid/base catalyzed reaction. In the initial step, a stock solution of TEOS, ethanol, H_2O, and HCl was combined in the molar ratio $1.0:11.3:17.2:1.4\times10^{-3}$ and refluxed at 60°C for 90 minutes. The stock solution was prepared with ultrapure Milli-Q water with resistivity > 18 MΩ-cm (Milli-Q-plus system, Millipore, Bedford, MA). In the second step, 0.5 M NH_4OH, stock solution, and ethanol were added in a volume ratio that varied with generation.

2.1. Indirect Synthesis and Characterization of Aerogel Films

During indirect synthesis, silica aerogel thin films were prepared in bulk.

2.1.1. Generation 1

Sample Preparation

Two batches of sol-gels were prepared during Generation 1 (G1). In the second step of sol-gel synthesis, a mixture of 0.5 M NH_4OH, stock solution, and ethanol reacted in the volume ratios 1:10:33 and 1:10:44. G1 gels formed and aged at 50°C for 48 hours, followed by a daily pore fluid-exchange of 100% ethanol, ethanol/hexane (3:1 v/v), ethanol/hexane (1:1 v/v), ethanol/hexane (1:3 v/v), and 100% hexane, respectively. These gels were then functionalized with 5 wt % TMCS in hexane at 60°C for 12 hours. After sonication with ultrasound for 1 hour, the functionalized gels were partially re-liquefied. 1 ml aliquots were spin-coated onto luster Al pin mounts (SPI Supplies) and silica sensors (Q-Sense) at a speed

of 2000 rpm for 15 seconds. The coated films were subcritically dried in hexane at room temperature for 12 hours, then analyzed using SEM.

Substrate Preparation

Aluminum pin mounts (12.7 mm in diameter) and silica sensors (0.2 cm^2 in area, 50 nm thick) were treated prior to film deposition. Silica sensors contain an active SiO_2 surface and are coated with an Au electrode (100 nm thick) on the opposite side. The AT-cut piezoelectric quartz crystals operated at 5 MHz and were optically polished with a root-mean-square roughness less than 3 nm. Aluminum stubs and sensors were oxidized by UV-Ozonation for 10 minutes, treated in 2 vol % Hellmanex solution (Hellma Co.) for 30 minutes, rinsed with de-ionized (DI) water, blown dry with air, and treated again with UV-Ozonation for 10 minutes.

SEM Preparation & Use

Before surface characterization by SEM, prepared silica sensors were mounted on specimen pin stubs with conductor tape. All samples were then pre-pumped at least 24 hrs before SEM use. Once the samples were clean and dry, they were inserted into the vacuum chamber for analysis.

A LEO 982 field emission scanning electron microscope (FE-SEM, Carl Zeiss SMT Inc., Peabody, Massachusetts) was used for surface characterization. Accelerating voltage was set at 5.0 kV for G1 films. The images were taken with a magnification of 50000× at working distances of 2 mm to 4 mm. As a side note, subsequent generations were imaged at 4.0 kV.

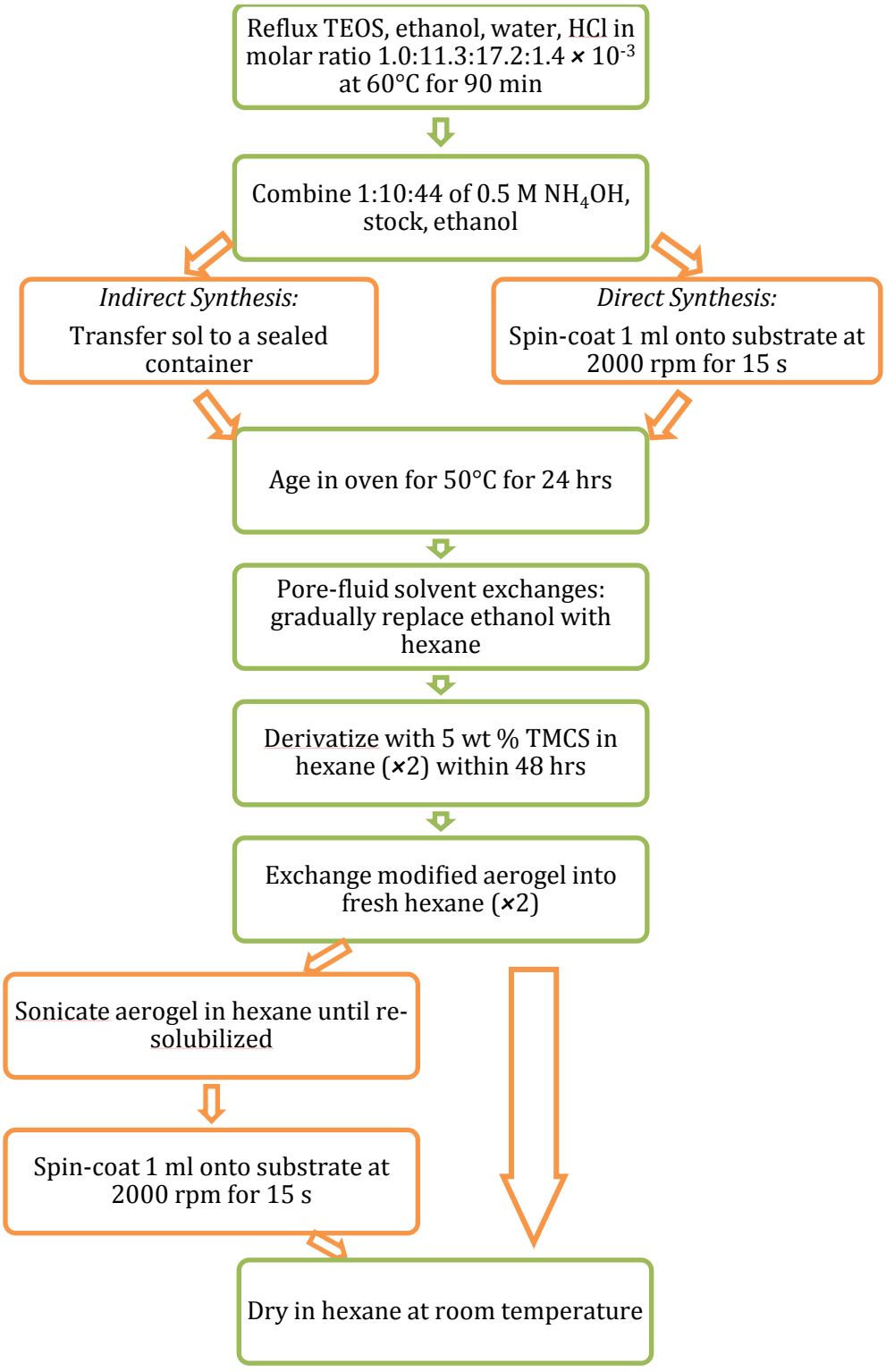

Figure 3. General experimental protocol for *indirect* (left) and *direct* (right) synthesis of silica aerogel thin films.

2.1.2. Generation 2

Two sets of bulk aerogels were produced during Generation 2 (G2). In the second step of sol-gel formation, 0.5 M NH_4OH, stock solution, and ethanol were added in volume ratios of 1:10:22 and 1:10:44. Unlike G1 conditions, G2 solvent washings occurred twice in one day when aerogels were transferred into a new solvent. These gels were then functionalized with 5 wt % TMCS in hexane for 12 hours at room temperature. G1 conditions for ultra-sonication and film deposition were repeated for G2 samples. Only sols formed with 44 ml ethanol were characterized using SEM.

2.1.3. Generation 3

G3 aerogels were prepared according to the protocol for G1 and G2 aerogels. In the second step of sol-gel formation, 0.5 M NH_4OH, stock solution, and ethanol were added in ratios of 1:10:33 and 1:10:44. G3 samples underwent the same number of solvent exchanges as G2 samples. Films were analyzed using SEM.

2.1.4. Generation 4

Sample Preparation

Based on the protocol for G2 aerogels, G4 samples were prepared with minor changes. The sols formed in 44 ml ethanol during two-step synthesis underwent two derivations with 4 wt % TMCS in hexane. These functionalized aerogels were exchanged into fresh hexane and placed in an ultra-sonic bath for 2 hours. The solutions were vigorously stirred and ultra-sonicated for another 30 minutes. Unlike previous generations, G4 sols were spin-coated onto octadecanethiol-functionalized Au QCM-D sensors (Q-Sense) and CZ p-Si<100> wafers (Virginia Semiconductor), placed in a partially closed container of hexane to

dry, and later characterized. Excess sol was also dried and stored in ambient conditions. The resulting aerogel was gently heated at 50ºC for 24 hours to induce "spring-back."[19]

Substrate Preparation

Gold sensors and silicon wafers were cleaned prior to use. Like the silica sensors used for G1 films, gold sensors (0.2 cm^2 in area, 50 nm thick) were AT-cut quartz crystal disks operating at 5 MHz and optically polished with a root-mean-square roughness less than 3 nm. These crystals, however, lacked a SiO_2 coating, leaving the Au electrode exposed to the analyte. Sensors were oxidized by UV-Ozonation for 10 minutes, treated with 1:1:5 30% hydrogen peroxide/concentrated ammonium hydroxide/water solution for 5 minutes, rinsed with water, blown dry with air, and thereafter decontaminated with UV-Ozonation before use. After the pre-cleaning procedure, Au sensors were immersed in a 10 mM octadecanethiol (ODT) / chloroform solvent overnight. ODT-gold crystals were subsequently soaked in ethanol, rinsed with pure water, and dried with air before QCM-D runs. Single-side polished silicon wafers (25.4 mm ± 0.3 mm in diameter, 250 μm ± 25 μm thick, resistivity ≤ 0.01 Ω-cm) were treated with the cleaning protocol used for aluminum stubs and silica sensors.

Ellipsometry

A Stokes Ellipsometer (Gaertner Scientific, Skokie, Illinois) was used to measure film thickness and refractive index. Measurements were taken at a shallow angle of incidence of 45º.[37] Five measurements were made for each sample. Refractive index of the silicon substrate was factored into spectroscopic calculations.

Gas-Phase Adsorption

With the help of students from the Advanced Physical Chemistry course, gas-phase adsorption was used to characterize the silica-based aerogel. A sample of 0.55 g was manually crushed and baked in the oven prior to the experiment. A vacuum line was calibrated and used to measure the amount of nitrogen gas adsorbed by the aerogel. Nitrogen gas adsorption occurred in incremental steps until the aerogel became saturated. Adsorption was then measured as a function of pressure, and the data was fit to a BET isotherm.

Emulsion Preparation

To simulate basic oil-contaminated water conditions, G4 films were exposed to one of two emulsions: w/o, a water-in-oil emulsion, and o/w, an oil-in-water emulsion.[38] The w/o emulsion was prepared from 80 wt % hexadecane and 20 wt % (1 wt % Tween 20) aqueous solution; the o/w emulsion was prepared from 20 wt % hexadecane and 80 wt % (1 wt % Tween 20) aqueous solution. These mixtures were ultra-sonicated for 7 minutes.

QCM-D

QCM-D (E4, Q-Sense, Gothenburg, Sweden) was used to collect real-time frequency and dissipation data. Cell temperature was set at 20°C for all QCM-D runs. Each flow cell was initially exposed to DI water as an internal control. After a stable baseline was established, the cell was introduced to either the w/o emulsion or o/w emulsion (Figure 4). The cell was flushed with DI water in the final step.

2.1.5. Generation 5

The protocol for fabricating G4 samples was repeated for G5 aerogels. One exception was that 5 wt % TMCS was used to derivatize the hydrophobic aerogel.

a)

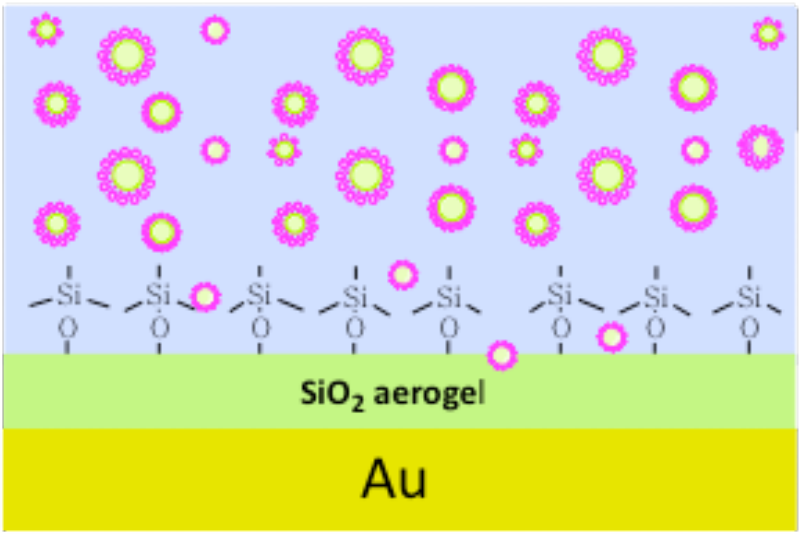

b)

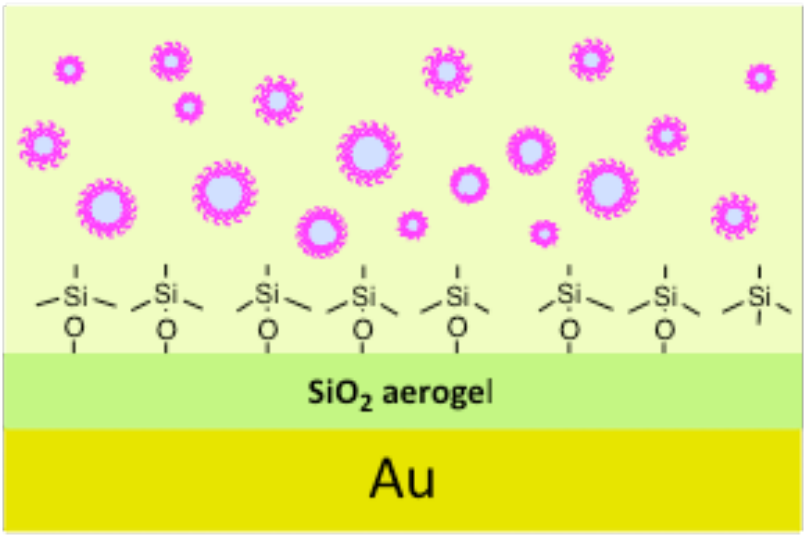

Figure 4. QCM-D experimental set-up for emulsions flowing through functionalized silica aerogel thin films deposited on a gold quartz sensor: a) o/w emulsion with 20 wt % hexadecane and 80 wt % (1 wt % Tween 20) aqueous solution, b) w/o emulsion with 80 wt % hexadecane and 20 wt % (1 wt % Tween 20) aqueous solution.

QCM-D Preparation & Use

Hydrophobic gold crystals were prepared as a control for QCM-D runs. Hexadecane, a major component of fuel oil, was the model oil for the QCM-D experiments. ODT-gold crystals were flushed with an anionic surfactant solution to remove possible contaminants. Surfactant sodium dodecyl sulfate (SDS) was re-crystallized in ethanol and then prepared in Milli-Q water at 10 mM SDS, a concentration well above its critical micelle concentration (CMC = 8.2 mM at 25°C).

After the surfactant was introduced and the system equilibrated, the control sensor was rinsed with water, hexadecane, and again with water. Although control conditions were repeated for the experiment, Tween 20 (1 wt % in pure water) was used.

2.2. Direct Synthesis of Aerogel Films

2.2.1. Isolated Module

Since the experimental conditions for indirect synthesis are not suitable for direct synthesis of a thin film sol-gel, we modified the protocol. During direct synthesis of aerogel films, we wanted to expose the sensor surface but protect the electrode. In essence, we wanted to mimic the set-up of a QCM-D standard flow cell. We therefore designed an isolated QCM-D module that only exposes the sensor surface to the atmosphere. The module itself is made of Delrin, a thermoplastic acetal resin that combines the advantageous properties of both metals and plastics.[39] As shown in Figure 5, this easily assembled and interchangeable module consists of two ends that are secured by three pins. The bottom piece contains a groove that fits two O-rings and a sensor. Once the module is assembled, the top piece, a hollow tube that encloses the surface of the sensor, forms a well with the bottom

piece. This well exposes the surface to approximately 1 ml of liquid. Due to the module's design, individual components can be replaced if necessary.

2.2.2. Generation 6

Unlike previous generations, Generation 6 aerogels were prepared directly on the substrates. After the two-step acid/base catalytic reaction, sol-gels were immediately spin-coated onto silicon wafers. Excess sol-gel was reserved and transformed into bulk aerogel via the indirect method for nitrogen sorption analysis. Subsequent gelation, aging, and solvent exchanges occurred as they had during direct synthesis, albeit on a smaller scale. After aging in the oven at 60ºC for 24 hours, wafers were stored in the solvent. Films were exposed to the same solvent mixture twice. Pore-fluid exchanges occurred daily. Surface derivatization occurred twice with 10 ml of 5 wt % TMCS in hexane. Films were dried in hexane under ambient conditions.

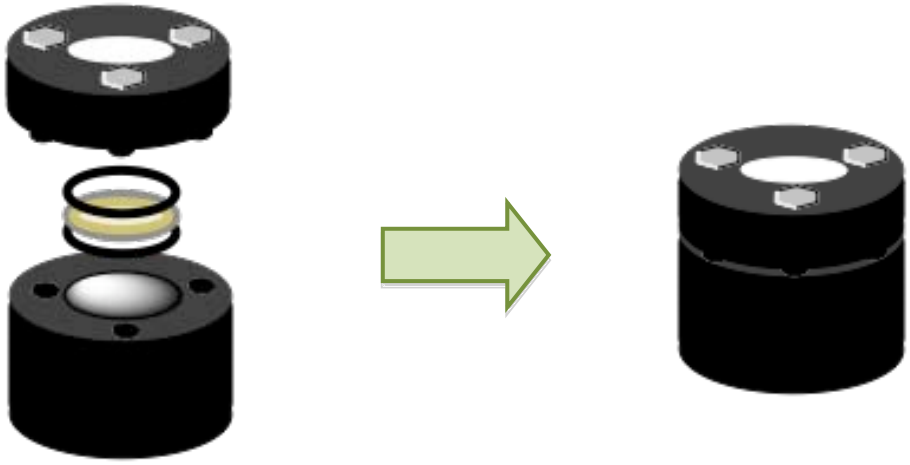

Figure 5. Schematic of isolated module. *Left:* individual components from top: top piece, O-ring, sensor, O-ring, bottom piece. *Right:* assembled module.

3. Results and Discussion

3.1. Indirect Synthesis and Characterization of Thin Films

3.1.1. Generation 1

Generation 1 (G1) aerogel films were partially synthesized and characterized. Upon sonication, neither alcogel from G1 successfully reverted into a sol. The alcogels prepared in the volume ratio 1:10:33 were more intact than those prepared in the volume ratio 1:10:44. On the mechanistic level, condensation reactions are inhibited as solvent content increases.[40] As observed in a rearranged version of [3], a newly formed siloxane bond is cleaved during alcoholysis to produce a silanol group and an alkoxide group:

$$(\mathrm{OR})_3\mathrm{Si}-\mathrm{O}-\mathrm{Si}(\mathrm{OR})_3 + \mathrm{ROH} \leftrightarrow (\mathrm{OR})_3\mathrm{Si}-\mathrm{OR} + \mathrm{HO}-\mathrm{Si}(\mathrm{OR})_3 \qquad [3a]$$

Since transesterification inhibits polymerization, the extensive silica network breaks down in the presence of increasing volumes of ethanol. Samples synthesized with a greater quantity of ethanol were mechanically weaker because they contained a higher liquid content.

Although silica aerogels contain various pores sizes, including macropores (50-1000 nm), mesopores (2-50 nm), and micropores (0.2-2 nm), they are primarily mesoporous and somewhat microporous.[25] G1 pore sizes and porous distribution were both smaller than expected. Characterization by SEM illustrated that films synthesized with 44 ml ethanol exhibited greater porosity and film consistency than those prepared with 33 ml ethanol. Since G1 samples prepared with 44 ml ethanol were less dense, they were more soluble and easier to spin-coat onto the substrate. Nevertheless, these films were not particularly consistent or mesoporous. While certain regions of a G1 film were quite porous, others were not. Macropores and mesopores dominated porous regions of the sample (Figure 6).

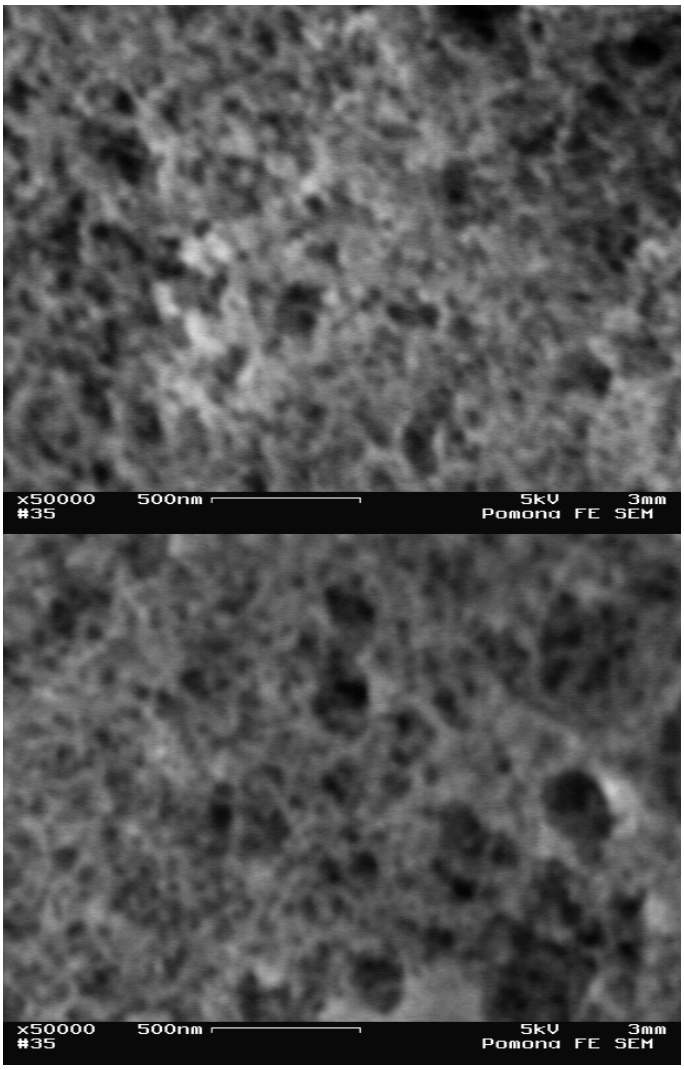

Figure 6. SEM images of macropores and mesopores observed in G1 samples at 50000× magnification. Films were prepared with 44 ml ethanol and spin-coated onto QCM gold sensors.

In regions with few pores, the sample surface was highly striated (Figure 7). Striations may have formed during film deposition of partially re-solubilized sol. An uneven film results when un-dissolved silica particulates are spin-coated onto the substrate.

Based on the SEM images, G1 samples lacked an interconnected porous silica network. The absence of an open pore network may be due to residual pore impurities. G1 aerogels underwent minimal solvent exchanges within a short time span. It is possible that

during the gradual transition into hexane solvent, impurities such as ethanol remained trapped inside the pores. As a result, contaminated pore surfaces may not have undergone complete derivation with hydrophobic TMCS. It is possible that the exposed hydrophilic pockets reacted with water vapor in the air after silylation. The compression forces that ensued would have collapsed the silica network and reduced the porosity of the aerogel.

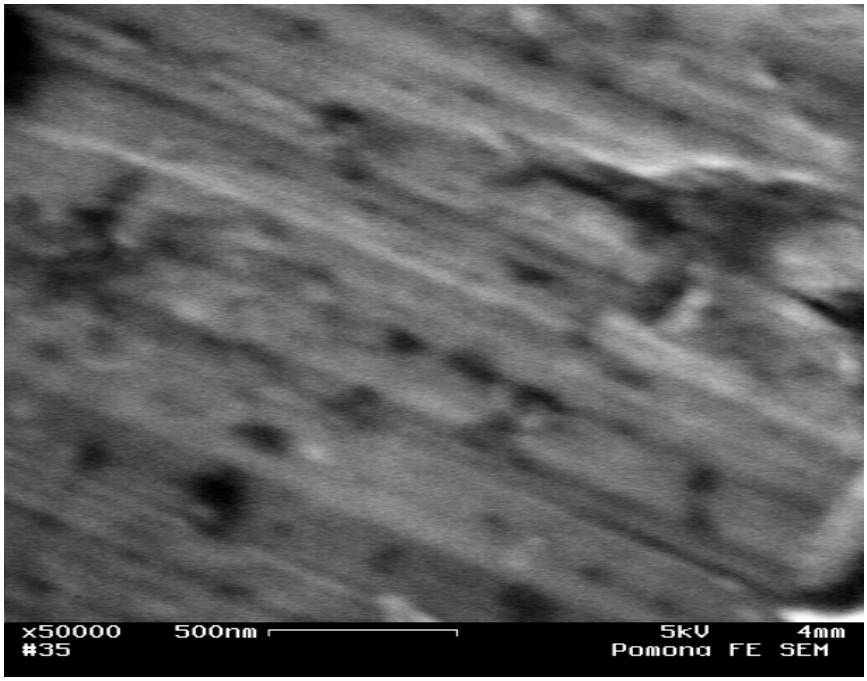

Figure 7. SEM image of a G1 silica aerogel film at 50000× magnification. Film was prepared with 44 ml ethanol, spin-coated onto an Al stub, and highly striated.

3.1.2. Generation 2

The sol-gel process was modified for Generation 2 (G2) films to improve their physical properties. Pore-fluid-exchanges increased in frequency. Pore structure of these aerogel films was more consistent with typical silica aerogel properties. As observed with G1 aerogels, a decrease in solvent content (22 ml) resulted in a denser alcogel. After 2 hours of ultra-sonication, samples prepared with 22 ml of solvent barely re-liquefied and were not used during spin-coating. Alcogels prepared with 44 ml of ethanol were less dense and easier

to re-solubilize. Unlike G1 samples, G2 films prepared from this sol-gel had smaller pore sizes. The extensive network of mesopores and few micropores observed in these aerogels is consistent with the pore sizes found in an ideal silica aerogel (Figure 8). Striations were minimal.

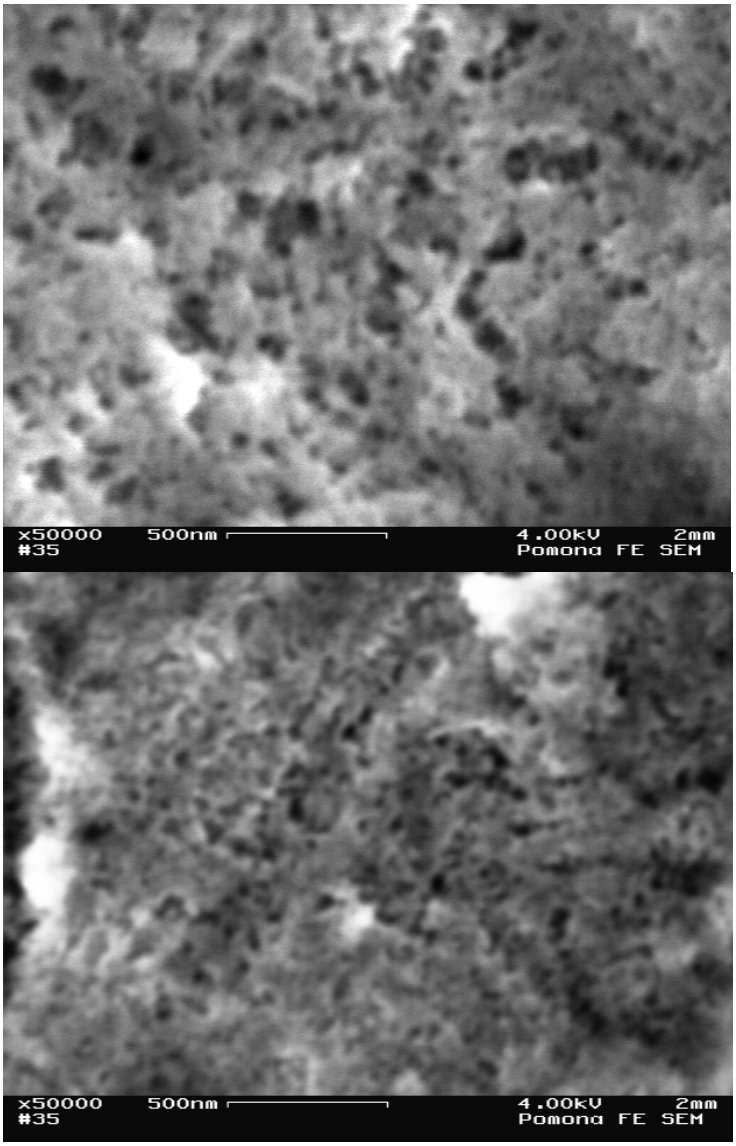

Figure 8. SEM images of G2 aerogel films at 50000× magnification. Films were prepared with 44 ml ethanol, spin-coated onto a QCM gold sensor, and mesoporous.

3.1.3. Generation 3

Both thin film deposition and film characterization were not possible for G3 samples, which remained as alcogels, even after more than 2 hours of sonication. A possibility is that a strong silica network may have formed. Prior to ultrasonication of future generations, gels were broken into smaller pieces to promote dissolution in hexane. During ultra-sonication, gels were also periodically removed and vigorously stirred to encourage the breakdown of the silica network.

3.1.4. Generations 4 and 5

Based on preliminary characterization by SEM, ellipsometry, gas-adsorption, and QCM-D, G4 samples exhibited properties of silica-based aerogels, which have a porosity ranging from 70 - 99%, pore diameters of approximately 50 nm, and a surface area of 600 to 1000 m^2 based on the nitrogen adsorption/desorption BET method.[25] G4 aerogels were the first samples to be characterized by multiple techniques because of their apparent uniformity and film consistency under SEM. Unlike other generations, G4 films were imaged at a magnification of 30000× due to instrument malfunction. The film surfaces contained minimal striation and an inter-porous silica network. Pore diameters ranged from ~40 nm to ~200 nm (Figure 9).

According to quantitative measurements made by SEM, thickness ranged from approximately 275 to 400 nm. Film thickness could only be crudely measured using SEM due to cross-section variability and cracking. The rough edges of the sample possibly formed after scoring the wafers. In this case, ellipsometry might be a more reliable technique for measuring thickness. Based on the measurement of unscored portions of the film, G4 aerogels on silicon wafers had a refractive index of 1.08 and a thickness of 287.00 ± 0.85 nm.

The refractive index is consistent with literature values (n =1.0 to 1.08).[25] Using the porosity-refractive index relation [4], G4 samples had a film porosity of 80.9%, an intermediate value for porosity.

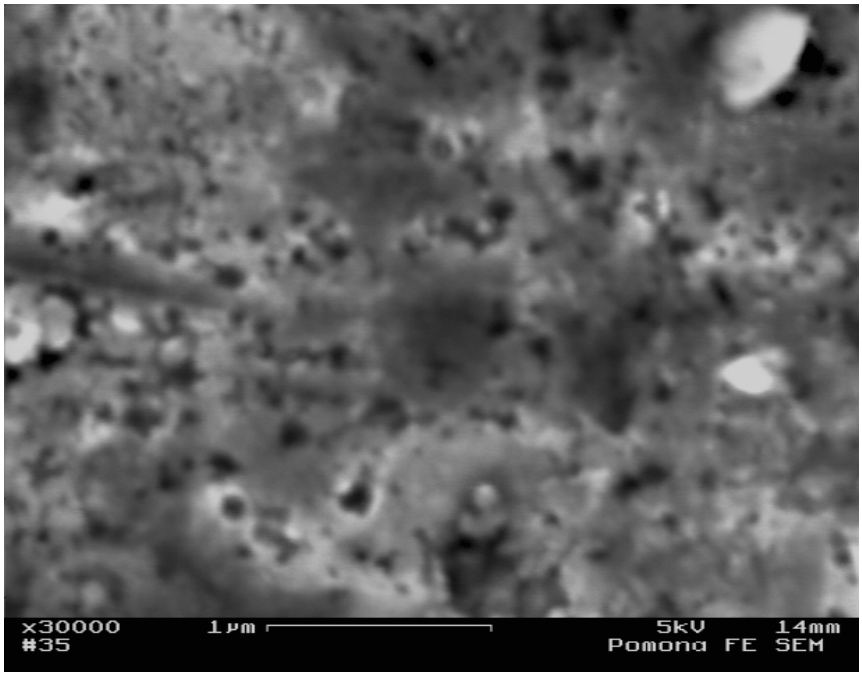

Figure 9. A SEM image of a spin-coated G4 silica-based aerogel film at 30000× magnification.

Not all methods of characterization were utilized for G5 films. Instead, these were prepared primarily for QCM-D experiments. Since we had verified the presence of a nanoporous silica network from previous generations of aerogels, SEM was not utilized to characterize the porous nature of G5 samples. On the other hand, film thickness and refractive index were not measured by ellipsometry because of difficulty obtaining readings. This was probably due to the increased light scattering on these thin aerogel film surfaces.[23]

Gas-Phase Adsorption

Based on intermediate relative pressures (when $p^* = 1$) found in the linear region of the BET isotherm, we determined the specific surface area for G4 aerogels. We used [5] to obtain a linear BET fit ($R^2 = 0.995$) for relative pressures between 0.16 and 0.32 (Figure 10). The y-intercept of the plot was 98.87 and the slope was 159.45. After relating the slope in terms of the y-intercept, we found that $c = 2.61$. The surface area of the G4 aerogel was 377.66 m^2/g, assuming that $\sigma = 0.162$ nm^2 for a nitrogen gas molecule.

In a similar study with TMCS-functionalized silica aerogels, Zhou determined specific surface areas less than our value.[41] Zhou *et al* used a one-step, acid-catalyzed sol-gel process, followed by derivatization with varying concentrations of TMCS/hexane solutions. He found that increasing the concentration of TMCS (~7.0 – 10.0 wt %) increased the specific surface area of the aerogel.[41]However, when Zhou applied 5 wt % TMCS, the surface area ($S = 258.35$ m^2/g) was less than ours ($S = 377.66$ m^2/g).

If we compare the two synthetic pathways, we can understand the discrepancy in surface area. Although we pursued a two-step sol-gel method, Zhou and his colleagues prepared their aerogel via a one-step, acid-catalyzed sol-gel process at room temperature.[41] An advantage to the two-step method is that the pre-polymerized sol formed during the reflux ($T = 60°C$) will undergo further condensation reactions in the second step. If handled carefully during solvent exchanges and surface functionalization, the aerogels fabricated by the two-step method would exhibit a complex, inter-porous network with a high surface area and narrow pore size distribution.

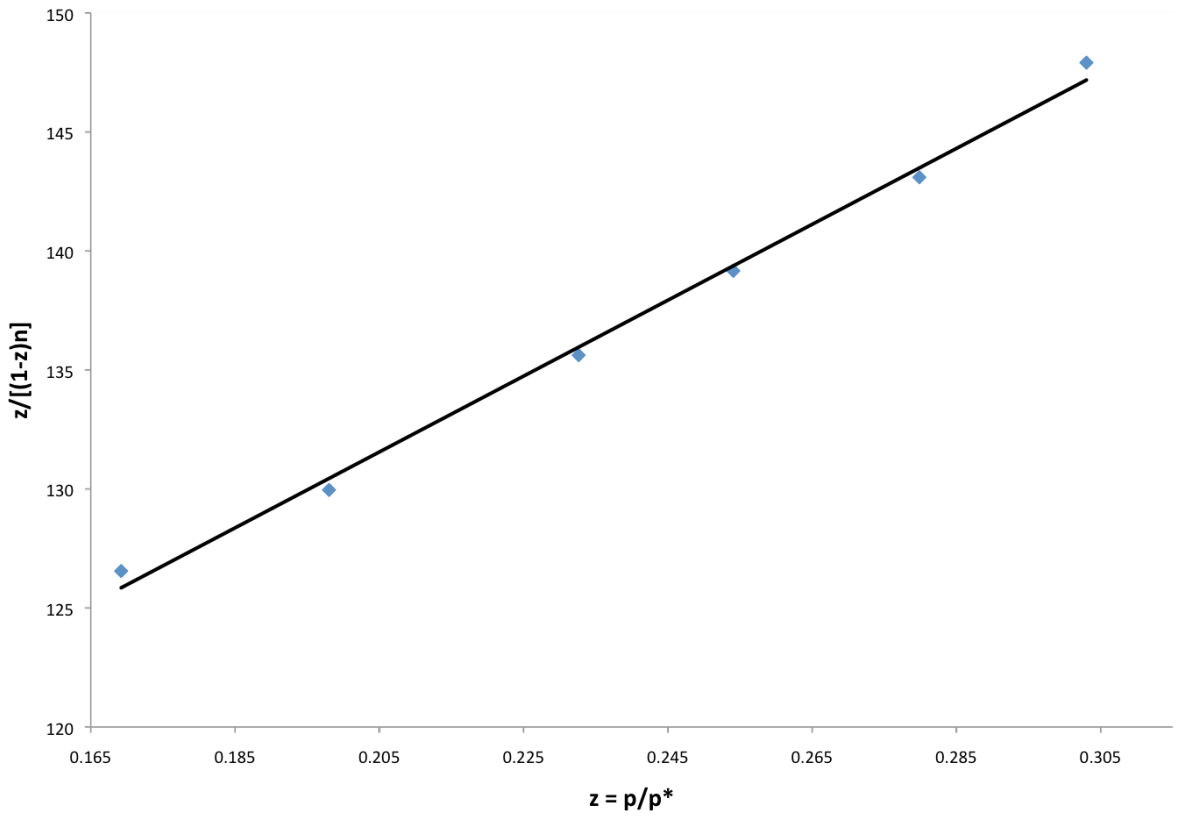

Figure 10. Plot of linearized BET adsorption isotherm for G4 aerogels at relative pressures between 0.16 and 0.32.

On the other hand, when we assessed higher BET surface area values (~1000 m^2/g) found for silica-based aerogels, our sample had a relatively low surface area.[25] A possible explanation for this difference is that surface silylation may not have reached completion in our samples. Unreacted surface silanol groups would be susceptible to condensation reactions. If this were the case, we could increase the hydrophobicity of the aerogel to inhibit further reactions. Another possibility is to identify the ideal concentration of TMCS (~7.0 – 10.0 wt %) for maximizing specific surface area.[41] Zhou determined that his samples achieved the largest surface area after exposure to ~8.6 wt % TMCS. Since our samples initially exhibited a different surface area than those synthesized in Zhou's study, we would expect the ideal concentration of TMCS to vary. Other methods for increasing surface area

include modifying the composition of the aerogel recipe, particularly the volume of ethanol, TEOS, and/or catalyst added.

QCM-D Oil Uptake

During initial QCM-D experiments with the coarse emulsions and pure hexadecane, we observed an unexpected positive frequency shift. "Desorption" of unknown material, presumably of the aerogel, seemed to occur. To simplify experimental conditions and isolate the cause of film "desorption," we repeated the experiment with pure hexadecane.

After simplifying the experimental conditions, we expected the following observations to occur. Once oil was introduced into the cell, we anticipated a large frequency drop. At this point, the alkane molecules would be attracted to the film surface due to the strong dispersion forces between the hexadecane molecules and the methyl groups on the aerogel surface. The subsequent water rinse should have little effect on the hexadecane contained in the pores because of water's polarity and the aerogel's non-polarity. Upon introduction of the surfactant, we expected an increase in frequency. As amphiphiles, surfactants can travel between the oil phase and water phase to extract oily residues. Since the hydrophile-lipophile-balance number (HLB) of Tween 20 is quite high (HLB = 16.7), it prefers the polar phase to the oil phase.[42] HLB numbers > 10 are hydrophilic, while HLB numbers < 10 are lipophilic.[42] The final water rinse should consequently remove any oil or surfactant residues trapped inside the aerogel pores and return the frequency to its initial value.

As a control, we exposed a pre-cleaned ODT-functionalized Au sensor to hexadecane. Upon exposure to the alkane, we observed a large frequency decrease (Δf = -

240 Hz). In comparison, the frequency decrease was notably less for an aerogel-coated ODT-Au sensor exposed to the same alkane (Δf = -53.8 Hz).

Due to the preliminary nature of the QCM-D experiment, we plotted frequency and dissipation shifts at the higher, ninth overtone (Figure 11). Given that frequency is inversely related to mass by the Sauerbrey relation [8], we determined a sensed mass of ~970.6 ng/cm^2 at the 9th overtone. Prior to oil exposure, the film was monitored in water and then in a surfactant solution. Tween 20 was used to maintain consistency with past experiments. During the wash with 1 wt % Tween 20 surfactant solution, frequency decreased until equilibrium was established. The dissipation response, which is sensitive to the viscous, or "floppy," nature of the film, mirrored the frequency response and increased until equilibrium was reached. Substrate exposure to the water rinse removed most of the surfactant solution and shifted the frequency back to the baseline (~0 Hz).

Frequency and dissipation values for the resonant and overtone frequencies (n = 1, 3, 5, 7, 9, and 11) deviated only after the sensor was exposed to hexadecane. The frequency shift (Δf = -53.8 Hz) was not nearly as large as the shift observed in the control (Δf = -240 Hz). During the adsorption process, dissipation increased from 0.5×10^{-6} to nearly 28×10^{-6}. The dissipation values indicate that the oil-aerogel system formed a loose, dissipative structure. The increase in energy dissipated by the film, as depicted by the differences among the various harmonics, signify the invalidity of the Sauerbrey relation. In cases where the Sauerbrey relation does not apply ($D > 1 \times 10^{-6}$), we must consider the viscoelastic properties of the oil-aerogel system. While we recognize the highly viscoelastic nature of the system, we have not adjusted the Sauerbrey mass due to the preliminary nature of the experiment.

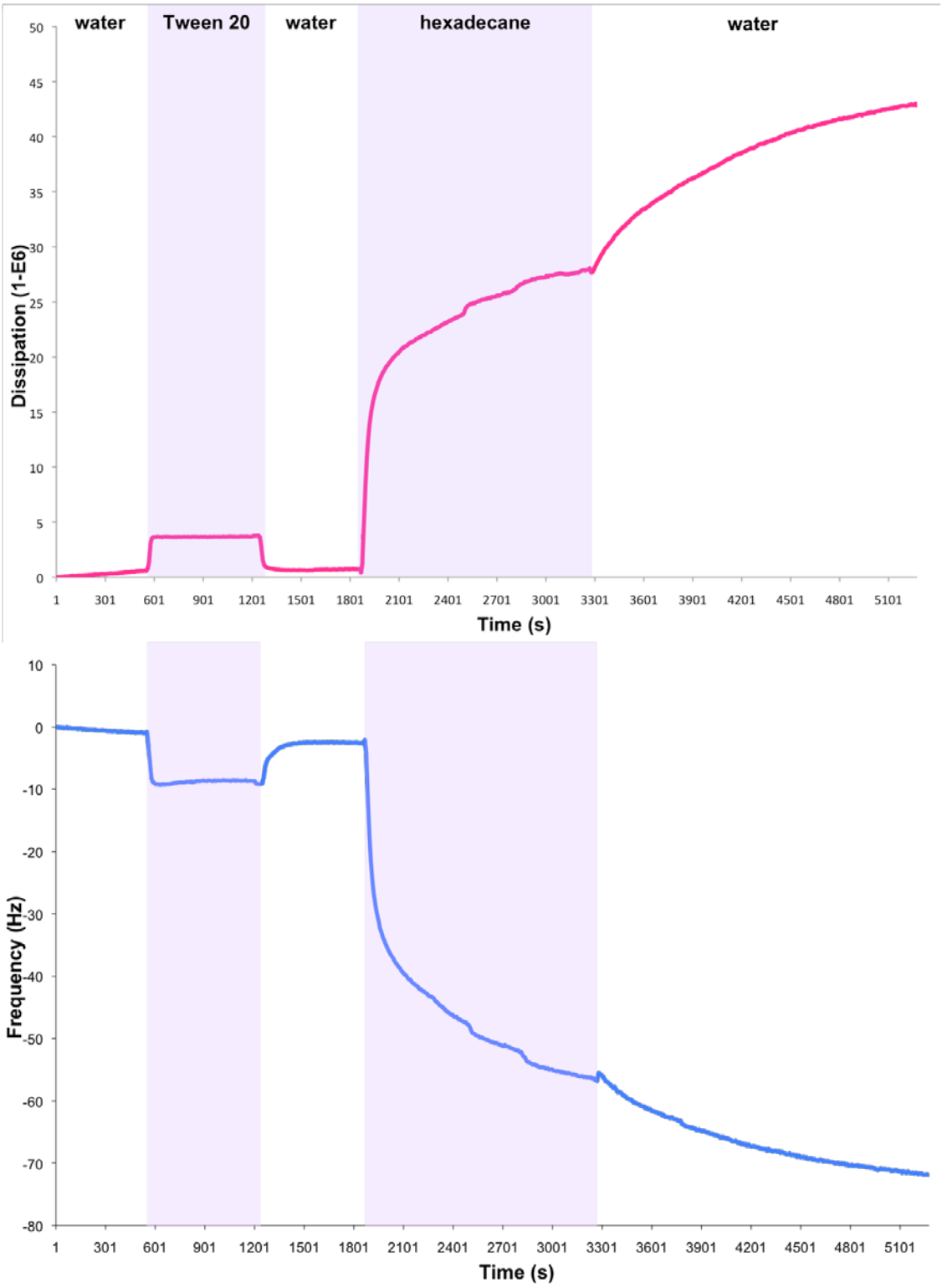

Figure 11. Adsorption of hexadecane onto an Au sensor coated with a TMCS-functionalized, silica-based aerogel. Time-resolved dissipation- *(top)* and frequency- *(bottom)* shifts for the 9th harmonic, as measured by QCM-D.

After the oil-aerogel system neared equilibrium, water was introduced to flush out unbound hexadecane molecules. We observed a continued decrease in frequency (Δf = -15.4 Hz) beyond the equilibrium level reached with hexadecane. Dissipation continued to increase, which indicates that hexadecane had adsorbed onto and into the porous aerogel.

A slight modification to this experiment would be to re-expose the sensor to the surfactant solution and a water rinse after the final step. The observed shifts in frequency and dissipation would elucidate information about continued aerogel oil uptake after exposure to surfactant solution. The water rinse should flush out oil droplets solubilized by the surfactant. If there is no significant frequency shift after film exposure to surfactant and water, then the oil has been trapped inside the aerogel pores.

Film Stability

In certain instances, frequency unexpectedly shifted above the baseline upon exposure to various fluids. The aerogel may have desorbed from the surface if it did not fully adhere to the ODT-gold substrate.

During film deposition, ODT-gold sensors may have been unevenly coated with the re-dispersed sol. The sol was re-liquefied in hexane, the non-polar solvent used to prime the sol-gel for surface derivatization with TMCS. According to Ruffner, hexane may not be the best solvent to use during spin-coating due to its high volatility.[24] During film deposition, hexane volatilizes from the surface at different rates as a result of factors such as temperature and concentration gradients.[24]

Heptane, a solvent with a lower volatility, could serve as a better alternative. Compared to the shorter hexane molecule, heptane has a longer carbon chain and a higher molecular weight. Heptane would therefore encounter stronger intermolecular forces, mainly

London dispersion forces that contribute to its stability as a liquid. Upon exposure to hexadecane, minimal, albeit QCM-D detectable, amounts of aerogel near the surface may have bound to the viscous, hydrophobic alkane chains. If we continue to observe "desorption" of material after replacing the solvent, we would need to investigate the robustness of the aerogel film itself.

A proposed method would be to isolate the effect of each variable QCM-D experimental protocol. First, we would monitor the film's stability in air. Before placing the sensor in the QCM-D, we would measure its refractive index using ellipsometry, assuming that it can be calculated. We would then flow air through the cell until the system equilibrates, remove the sensor, and measure its refractive index. If the refractive index were constant before and after the QCM-D run, the isolated variable is probably not responsible for the supposed film degradation. To test the effect of water, we would rinse the sensor with water, characterize it with ellipsometry, load the sensor into the QCM-D, expose it to water until the system equilibrates, and finally remove the sensor for another ellipsometric measurement. If the sensor were stable in air and water, we could then repeat the protocol with one of three variables: hexadecane, 1 wt % Tween 20, or an emulsion. Depending on the outcome of this methodical approach, it may be possible to determine the source of supposed film desorption.

3.2. Future Work with Direct Method

Aside from minor cases of material "desorption," a disadvantage of indirect synthesis is the notable accumulation of solvent waste, a practice that contradicts our overall goal to reduce detrimental environmental impacts of oil recovery techniques. After preliminary fabrication of these films, we experimented with the direct synthesis of thin films onto QCM-

D sensors. Certain challenges would need to be addressed before we can successfully use this method to directly fabricate and characterize thin aerogel films.

One of the advantages of direct synthesis is the significant reduction in solvent waste. Although aerogels are easier to manage in bulk, a considerable amount of solvent is required. Indirect synthesis reduces waste by ten-fold. Less TMCS, along with ethanol and hexane, enters the chemical waste stream. Since there is less surface area for thin films, we could strengthen the silica network by increasing the oven temperature during gelation and aging. However, if we were to raise the temperature, we would also need to consider the impact of using volatile solvents such as hexane.

Constructing multiple isolated modules would facilitate direct aerogel film synthesis onto QCM-D sensors in the future. Since the QCM-D contains four flow cells, these modules could be constructed in groups of four or five to ensure that at least four sensors are always prepared simultaneously. These modules would need to be modified with an airtight cap to ensure that highly volatile solvents remain in the well. Unless the well is tightly sealed from the atmosphere, hexane would rapidly volatilize during pore-fluid exchanges. An alternative is to use a lower volatility solvent during the washings.

Additionally, we would need to construct a removable, seal-proof cap to confine the solvent inside the isolated module. Future work on direct synthesis of thin films would need to consider the high vapor pressure of the solvents used prior to surface modification.

3.3 Conclusions

In this study, we pursued the indirect synthesis and initial characterization of hydrophobic silica aerogel films. The specific surface area (377.66 m^2/g), refractive index (1.08), and porosity (80.9%) were consistent with values in the literature. Using QCM-D, we determined that hexadecane, our model oil, adhered to the porous film after a water rinse. Since increasing aerogel porosity would maximize the surface area for oil uptake, future experiments should strive to produce films with $\pi > 90.0\%$. By altering the aerogel recipe, it is possible to obtain the desired physical and chemical properties. Due to their high porosity and low density, aerogel thin films are challenging to characterize with accuracy. It is important to recognize that different methods of characterization will yield different quantitative values. Although there are advantages and disadvantages to each method of characterization, we have attempted to utilize four widely used analytical techniques.[25] By improving the stability and reproducibility of the aerogel thin film, we may obtain QCM-D information about its oil absorbing capacity and its viscoelastic properties. A potential alternative to the indirect method is to explore the direct synthesis of thin films onto QCM-D sensors, a promising approach that would reduce the environmental impact of the aerogel waste stream. As demonstrated in this study, preliminary QCM-D analysis of synthesized hydrophobic aerogel thin films is possible and can be further explored to better understand and improve the oil-sorbent capabilities of such unique materials.

Acknowledgements

I would like to thank Dr. Malkiat S. Johal for his continued guidance and support throughout this process. Additionally, I would like to thank David Haley for his assistance and expertise with the SEM, as well as students from the Advanced Physical Chemistry for conducting the gas sorption experiments. Lastly, I would like to thank the Department of Chemistry and the Department of Physics for supplying the resources and materials for my thesis.

References

[1] National Wildlife Federation. Oil Spill Crisis. http://www.nwf.org/Oil-Spill/Effects-On-Wildlife/Compare-Exxon-Valdez-and-BP-Oil-Spills.aspx (accessed Nov. 28, 2010).

[2] Adebajo, M.O.; Frost, R.L.; Kloprogge, J.T.; Carmody, O.; Kokot, S. *J. Porous Mat.* **2003**, *10*, 159-170.

[3] Ghalambor, A. *The Effectiveness of Solidifiers for Combating Oil Spills*; OSRADP Technical Report Series 96-006; Louisiana Applied Oil Spill Research and Development Program: 1997.

[4] Choi, H.M.; Cloud, R.M. *Environmental Science and Technology* **1992**, *26*, 772.

[5] Gurav, J.L.; Jung, I.K.; Park, H.H.; Kang, E.S.; Nadargi, D.Y. *J. Nanomater.* **2010**, *2010*, 11.

[6] Fricke, J.; Tillotson, T. *Thin Solid Films* **1997**, *297*, 212-223.

[7] Kistler, S.S. *J. Phys. Chem.* **1932**, *36*, 52-64.

[8] Fricke, J.; Emmerling, A. *Struct. Bonding* **1992**, *77*, 37.

[9] Yoldas, B.E.; Annen, M.J.; Bostaph, J. *Chem. Mater.* **2000**, *12*, 2475.

[10] Gross, J.; Fricke, J.; Hrubesh, L.W. *J. Acoust. Soc. Am.* **1992**, *91*, 2004.

[11] Hair, L.M.; Coronado, P.R.; Reynolds, J.G. *J. Non-Crystl. Solids* **2000**, *279*, 115.

[12] Aelion, R.; Loebel, A.; Eirich, F. *J. Am. Chem. Soc.* **1950**, *72*, 5705.

[13] Sakka, S. in Aegerter, M.A.; Jafelicci Jr. M.; Souza D.F.; Zanotto, E.D. *Sol Gel, Science and Technology* **1989**, World Scientific, Singapore, 76-102.

[14] Liu, M.; Yang, D.; Qu, Y. *J. Non-Cryst. Solids* **2008**, *354*, 4927-4931.

[15] Rao, A.V.; Bhagat, S.D. *Solid State Sciences* **2004**, *6*, 945-952.

[16] Iler, R.K. *The Chemistry of Silica* **1979**, John Wiley, New York.

[17] Despetis, F.; Etienne, P.; Etienne-Calas, S. *J. Non-Cryst. Solids* **2004**, *344*, 22-25.

[18] Kistler, S.S.; *Nature* **1931**, *127*, 741.

[19] Prakash, S.S.; Brinker, C.J.; Hurd, A.J. *J. Non-Cryst. Solids* **1995**, *190*, 264-275.

[20] Brinker, C.J.; Scherer, G.W. *Sol-Gel Science: The Physics and Chemistry of Sol-Gel Processing* **1990**, Academic Press, San Diego, Calif, USA.

[21] Pierre, A.C.; Pajonk, G.M. *Chem. Rev.* **2002**, *102*, 4243-4265.

[22] Shen, J.; Zhang, Z.; Wu, G.; Zhou, B.; Ni, X.; Wang, J. *J. Mater. Sci.* **2006**, *22*, 798-802.

[23] Kim, G.S.; Hyun, S.H. *Thin Solid Films* **2004**, *460*, 190-200.

[24] Ruffner, J.A.; Clem, P.G.; Tuttle, B.A.; Brinker, C.J.; Warren, W.L.; Schwartz, R.W.; Raymond, M.V.; Al-Shareef, H.N.; Mortimer, D.M.; Nasby, R.D.; Hurd, A.J.; Reichert, T.L.; Sriram, C.S.; Bhatia, R.; Bullington, J.A. *Sandia Report* **1998**, Sandia National Laboratories, Albuquerque, New Mexico, USA.

[25] Dorcheh, A.S.; Abbasi, M.H. *J. Mater. Sci.* **2008**, *199*, 10-26.

[26] Langmuir, I. *J. Am. Chem. Soc.* **1916,** *38*, 221-95.

[27] Brunauer, S.; Emmett, P. H.; Teller, E. *J. Am. Chem. Soc*. **1938**, *60*, 309-319.
[28] Sauerbrey, G. Z. *Phys.* **1959**, *155*, 206.
[29] Voinova, M.V.; Rodahl, M.; Jonson, M.; Kasemo, B. *Phys. Scr.* **1999**, *59*, 391–396.
[30] Weng, K.C.; Stalgren, J.R.; Duval, D.J.; Risbud, S.H.; Frank, C.W. *Langmuir* **2004**, *20*, 7232-7239.
[31] Reynolds, J.G.; Coronado, P.R.; Hrubesh, L.W. *J. Non-Cryst. Solids* **2001**, *292*, 127-137.
[32] Rao, A.V.; Hegde, N.D.; Hirashima, H. *J. Colloid Interface Sci.* **2007**, *305*, 124-132.
[33] Hrubesh, L.W.; Coronado, P.R.; Satcher, J.H. *J. Non-Cryst. Solids* **2001**, *285*, 328.
[34] Lee, C.J.; Kim, G.S.; Hyun, S.H. *J. Mater. Sci.* **2002**, *37*, 2237.
[35] McClements, D.J.; Dungan, S.R. *J. Phys. Chem.* **1993**, *97*, 7304-7308.
[36] Elam, J.W.; Pellin, M.J. *Anal. Chem.* **2005**, *77*, 3531-3535.
[37] Kim, G.S.; Hyun, S.H. *Thin Solid Films* **2003**, *460*, 190-200.
[38] McClements, D.J.; Dungan, S.R. *J. Phys. Chem.*, **1993**, *97(28)*, 7304-7308.
[39] DuPont. Acetal Resin: Delrin. http://www2.dupont.com/Plastics/en_US/Products/Delrin/Delrin.html (accessed April 10, 2011).
[40] Sinko, K. *Materials* **2010**, *3*, 704-740.
[41] Zhou, X.C.; Zhong, L.P.; Xu, Y.P. *Inorganic Materials*, **2008**, *44*, 976-979.
[42] Sigma-Aldrich. Surfactants Classified by HLB Numbers. http://www.sigmaaldrich.com/materials-science/material-science-products.html?TablePage=22686648 (accessed April 18, 2011).